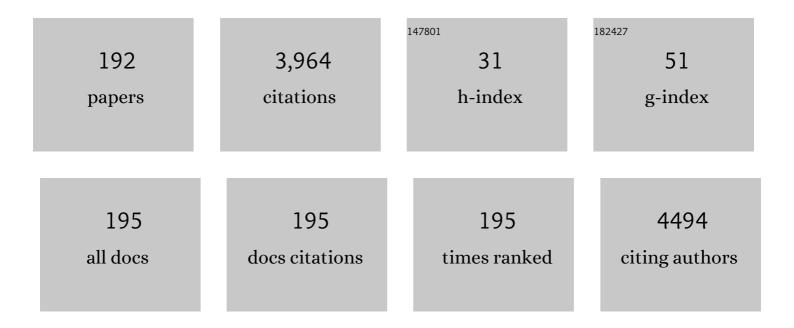
Duane Choquesillo-Lazarte

List of Publications by Year in descending order

Source: https://exaly.com/author-pdf/5783069/publications.pdf Version: 2024-02-01



#	Article	IF	CITATIONS
1	Guest Molecule-Responsive Functional Calcium Phosphonate Frameworks for Tuned Proton Conductivity. Journal of the American Chemical Society, 2014, 136, 5731-5739.	13.7	206
2	Multifunctional Luminescent and Proton-Conducting Lanthanide Carboxyphosphonate Open-Framework Hybrids Exhibiting Crystalline-to-Amorphous-to-Crystalline Transformations. Chemistry of Materials, 2012, 24, 3780-3792.	6.7	162
3	Intramolecular "Arylâ^'Metal Chelate Ringâ€i€,Ĩ€-Interactions as Structural Evidence for Metalloaromaticity in (Aromatic α,αâ€`-Diimine)â^'Copper(II) Chelates: Molecular and Crystal Structure of Aqua(1,10-phenanthroline)(2-benzylmalonato)copper(II) Three-hydrate. Inorganic Chemistry, 2002, 41, 6956-6958.	4.0	108
4	Versatile synthesis and enlargement of functionalized distorted heptagon-containing nanographenes. Chemical Science, 2017, 8, 1068-1074.	7.4	100
5	Tiâ€Catalyzed Barbierâ€Type Allylations and Related Reactions. Chemistry - A European Journal, 2009, 15, 2774-2791.	3.3	93
6	Three new modes of adenine-copper(II) coordination: interligand interactions controlling the selective N3-, N7- and bridging μ-N3,N7î—,metal-bonding of adenine to different N-substituted iminodiacetato-copper(II) chelates. Inorganica Chimica Acta, 2002, 339, 160-170.	2.4	88
7	Stapled helical o-OPE foldamers as new circularly polarized luminescence emitters based on carbophilic interactions with Ag(<scp>i</scp>)-sensitivity. Chemical Science, 2016, 7, 5663-5670.	7.4	84
8	Tuning Proton Conductivity in Alkali Metal Phosphonocarboxylates by Cation Size-Induced and Water-Facilitated Proton Transfer Pathways. Chemistry of Materials, 2015, 27, 424-435.	6.7	82
9	Switchable Surface Hydrophobicity–Hydrophilicity of a Metal–Organic Framework. Angewandte Chemie - International Edition, 2016, 55, 16049-16053.	13.8	76
10	Interligand interactions involved in the molecular recognition between copper(II) complexes and adenine or related purines. Coordination Chemistry Reviews, 2008, 252, 1241-1256.	18.8	72
11	Intramolecular "CH··Â-Ï€(Metal Chelate Ring) Interactions―as Structural Evidence for Metalloaromaticity in Bis(pyridine-2,6-diimine)RullComplexes. European Journal of Inorganic Chemistry, 2005, 2005, 1585-1588.	2.0	65
12	Interligand Interactions Controlling the μ-N7,N9-Metal Bonding of Adenine (AdeH) to theN-Benzyliminodiacetato(2â^') Copper(II) Chelate and Promoting the N9 versus N3 Tautomeric Proton Transfer: Molecular and Crystal Structure of [Cu2(NBzIDA)2(H2O)2(μ-N7,N9-Ade(N3)H)]·3H2O. Inorganic Chemistry, 2002, 41, 6190-6192.	4.0	62
13	Synthesis, Structure, and Catalytic Applications for <i>ortho</i> and <i>meta</i> -Carboranyl Based NBN Pincer-Pd Complexes. Inorganic Chemistry, 2014, 53, 9284-9295.	4.0	57
14	X-ray and NMR Crystallography Studies of Novel Theophylline Cocrystals Prepared by Liquid Assisted Grinding. Crystal Growth and Design, 2015, 15, 3674-3683.	3.0	57
15	Luminescent and Proton Conducting Lanthanide Coordination Networks Based On a Zwitterionic Tripodal Triphosphonate. Inorganic Chemistry, 2016, 55, 7414-7424.	4.0	57
16	A Highly Water-Stable <i>meta</i> -Carborane-Based Copper Metal–Organic Framework for Efficient High-Temperature Butanol Separation. Journal of the American Chemical Society, 2020, 142, 8299-8311.	13.7	54
17	A Windmill-Shaped Hexacopper(II) Molecule Built Up by Template Core-Controlled Expansion of Diaquatetrakis(I¼2-adeninato-N3,N9)dicopper(II) with Aqua(oxydiacetato)copper(II). Inorganic Chemistry, 2006, 45, 877-882.	4.0	51
18	Design, synthesis and biological evaluation of chalconyl blended triazole allied organosilatranes as giardicidal and trichomonacidal agents. European Journal of Medicinal Chemistry, 2016, 108, 287-300.	5.5	47

#	Article	IF	CITATIONS
19	Inter-ligand interactions and the selective formation of the unusual metal–N3(adenine) bond in ternary copper(II) complexes with N -benzyliminodiacetato(2â~) ligands. Inorganic Chemistry Communication, 2002, 5, 800-802.	3.9	46
20	A critical look on the nature of the intra-molecular interligand π,π-stacking interaction in mixed-ligand copper(ii) complexes of aromatic side-chain amino acidates and α,α′-diimines. CrystEngComm, 2004, 6, 627-632.	2.6	46
21	Structure, magnetism and DFT studies of dinuclear and chain complexes containing the tetrazolate-5-carboxylate multidentate bridging ligand. Dalton Transactions, 2009, , 6335.	3.3	44
22	Metal ion binding modes of hypoxanthine and xanthine versus the versatile behaviour of adenine. Coordination Chemistry Reviews, 2012, 256, 193-211.	18.8	41
23	New (RS)-benzoxazepin-purines with antitumour activity: The chiral switch from (RS)-2,6-dichloro-9-[1-(p-nitrobenzenesulfonyl)-1,2,3,5-tetrahydro-4,1-benzoxazepin-3-yl]-9H-purine. European Journal of Medicinal Chemistry, 2011, 46, 249-258.	5.5	39
24	Sulfoxideâ€Induced Homochiral Folding of <i>ortho</i> â€Phenylene Ethynylenes (<i>o</i> â€OPEs) by Silver(I) Templating: Structure and Chiroptical Properties. Chemistry - A European Journal, 2018, 24, 2653-2662.	3.3	38
25	Classical hydrogen bonding and stacking of chelate rings in new copper(<scp>ii</scp>) complexes. Dalton Transactions, 2017, 46, 2803-2820.	3.3	37
26	Synthesis and Anticancer Activity of (<i>R</i> , <i>S</i>)â€9â€(2,3â€Dihydroâ€1,4â€Benzoxathiinâ€3â€ylmethyl)â€9 <i>H</i> â€Purines. ChemMedCh 127-135.	em a, 22008,	336
27	Carborane Bis-pyridylalcohols as Linkers for Coordination Polymers: Synthesis, Crystal Structures, and Guest-Framework Dependent Mechanical Properties. Crystal Growth and Design, 2017, 17, 846-857.	3.0	36
28	Thermal assisted self-organization of calcium carbonate. Nature Communications, 2018, 9, 5221.	12.8	35
29	Design of cost-efficient and photocatalytically active Zn-based MOFs decorated with Cu ₂ O nanoparticles for CO ₂ methanation. Chemical Communications, 2019, 55, 10932-10935.	4.1	34
30	Metal chelates of N-(2-pyridylmethyl)iminodiacetate(2-) ion (pmda). Part I. Two mixed-ligand copper(II) complexes of pmda with N,N-chelating bases. Synthesis, crystal structure and properties of H2pmda·0.5H2O, [Cu(pmda)(pca)]·3H2O (pca=α-picolylamine) and [Cu(pmda)(Hpb)]·5H2O (Hpb=2-(2′-pyridyl)benzimidazole). Polyhedron, 2002, 21, 1485-1495.	2.2	33
31	Medium benzene-fused oxacycles with the 5-fluorouracil moiety: synthesis, antiproliferative activities and apoptosis induction in breast cancer cells. Tetrahedron, 2003, 59, 5457-5467.	1.9	33
32	An aqua-adenine H-bonding interaction controlling the formation of the rare Zn(II)–N9(adenine) bond in crystal structure of diaqua(adenine)(iminodiacetato)zinc(II). Inorganic Chemistry Communication, 2003, 6, 1354-1357.	3.9	32
33	Common Structural Features in Calcium Hydroxyphosphonoacetates. A High-Throughput Screening. Crystal Growth and Design, 2011, 11, 1713-1722.	3.0	32
34	Crystal engineering in confined spaces. A novel method to grow crystalline metal phosphonates in alginate gel systems. CrystEngComm, 2012, 14, 5385.	2.6	32
35	Cation Exchange Strategy for the Encapsulation of a Photoactive CO-Releasing Organometallic Molecule into Anionic Porous Frameworks. Inorganic Chemistry, 2016, 55, 6525-6531.	4.0	32
36	Versatile Bottomâ€up Approach to Stapled Ï€â€Conjugated Helical Scaffolds: Synthesis and Chiroptical Properties of Cyclic <i>o</i> â€Phenylene Ethynylene Oligomers. Angewandte Chemie - International Edition, 2012, 51, 13036-13040.	13.8	31

#	Article	IF	CITATIONS
37	Self-sacrificial MOFs for ultra-long controlled release of bisphosphonate anti-osteoporotic drugs. Chemical Communications, 2020, 56, 5166-5169.	4.1	31
38	A new bis-3-hydroxy-4-pyrone as a potential therapeutic iron chelating agent. Effect of connecting and side chains on the complex structures and metal ion selectivity. Journal of Inorganic Biochemistry, 2014, 141, 132-143.	3.5	30
39	Ti(III)-Catalyzed Cyclizations of Ketoepoxypolyprenes: Control over the Number of Rings and Unexpected Stereoselectivities. Journal of the American Chemical Society, 2014, 136, 6943-6951.	13.7	30
40	Synthesis, characterization, electronic absorption and antimicrobial studies of N-(silatranylpropyl)phthalimide derived from phthalic anhydride. Inorganica Chimica Acta, 2015, 427, 232-239.	2.4	30
41	Anhydrous Lithium Acetate Polymorphs and Its Hydrates: Three-Dimensional Coordination Polymers. Crystal Growth and Design, 2011, 11, 1021-1032.	3.0	29
42	From monomers to polymers: steric and supramolecular effects on dimensionality of coordination architectures of heteroleptic mercury(<scp>ii</scp>) halogenide–tetradentate Schiff base complexes. CrystEngComm, 2015, 17, 3493-3502.	2.6	29
43	Halogen bonded cocrystals of active pharmaceutical ingredients: pyrazinamide, lidocaine and pentoxifylline in combination with haloperfluorinated compounds. CrystEngComm, 2017, 19, 5293-5299.	2.6	29
44	Searching for new aluminium chelating agents: A family of hydroxypyrone ligands. Journal of Inorganic Biochemistry, 2014, 130, 112-121.	3.5	28
45	Ring–ring or nitro-ring π,π-interactions in N-(p-nitrobenzyl)iminodiacetic acid (H2NBIDA) and mixed-ligand copper(II) complexes of NBIDA and imidazole (Him), 2,2′-bipyridine (bipy) or 1,10-phenanthroline (phen). Crystal structures of H2NBIDA, [Cu(NBIDA)(Him)(H2O)], [Cu(NBIDA)(bipy)]·3H2O and [Cu(NBIDA)(phen)]·2H2O. Polyhedron. 2003. 22. 1039-1049.	2.2	27
46	Thiodiacetato-copper(II) chelates with or without N-heterocyclic donor ligands: molecular and/or crystal structures of [Cu(tda)]n, [Cu(tda)(Him)2(H2O)] and [Cu(tda)(5Mphen)]·2H2O (Him=imidazole,) Tj ET	QqQ2Q40 rg	BT Øverlock
47	Metal ion binding patterns of acyclovir: Molecular recognition between this antiviral agent and copper(II) chelates with iminodiacetate or glycylglycinate. Journal of Inorganic Biochemistry, 2011, 105, 616-623.	3.5	27
48	A family of hydroxypyrone ligands designed and synthesized as iron chelators. Journal of Inorganic Biochemistry, 2013, 127, 220-231.	3.5	27
49	Hydroxypyridinones with enhanced iron chelating properties. Synthesis, characterization and in vivo tests of 5-hydroxy-2-(hydroxymethyl)pyridine-4(1H)-one. Dalton Transactions, 2016, 45, 6517-6528.	3.3	27
50	Synthesis and characterization of modified Schiff base silatranes (MSBS) via â€~Click Silylation'. Journal of Molecular Structure, 2015, 1079, 173-181.	3.6	26
51	Three new tetranuclear phenoxy-bridged metal(II) complexes: Synthesis, structural variation, cryomagnetic properties, DFT study and antiprolifirative properties. Polyhedron, 2019, 161, 198-212.	2.2	26
52	Structural correlations in nickel(II)–thiodiacetato complexes: molecular and crystal structures and properties of [Ni(tda)(H2O)3]. Inorganic Chemistry Communication, 2004, 7, 1277-1280.	3.9	25
53	Divalent Metal Vinylphosphonate Layered Materials: Compositional Variability, Structural Peculiarities, Dehydration Behavior, and Photoluminescent Properties. Inorganic Chemistry, 2011, 50, 11202-11211.	4.0	25
54	A Racemic and Enantiopure Unsymmetric Diiron(III) Complex with a Chiral <i>o</i> arboraneâ€Based Pyridylalcohol Ligand: Combined Chiroptical, Magnetic, and Nonlinear Optical Properties. Chemistry - A European Journal, 2014, 20, 1081-1090.	3.3	25

#	Article	IF	CITATIONS
55	Spectral, structural, and superoxide dismutase activity of some octahedral nickel(II) complexes with tri-tetradentate ligands. Journal of Coordination Chemistry, 2010, 63, 3648-3661.	2.2	24
56	New copper(II) compound having protonated forms of ethylenediaminetetraacetate(4â^') ion (EDTA) and adenine (AdeH): synthesis, crystal structure, molecular recognition and physical properties of (AdeH2)[Cu(HEDTA)(H2O)]·2H2O. Polyhedron, 2002, 21, 1451-1457.	2.2	22
57	Synthesis, crystal structure and properties of N-tert-butyliminodiacetic acid (H2TEBIDA), [Cu(TEBIDA)(H2O)2], {[Cu(TEBIDA)(Him)]·2H2O}n, {Cu(TEBIDA) (5MeHim)·H2O}n, and [Cu(TEBIDA)(2,2′-bipy)(H2O)]·4.5H2O, (Him=imidazole, 5MeImH=5-methylimidazole and) Tj ETQq1 1 0.7843	147gBT /C) Verlock 10
58	Poly(ethylene) oxide for small-molecule crystal growth in gelled organic solvents. Journal of Applied Crystallography, 2011, 44, 172-176.	4.5	22
59	<i>m</i> -Carboranylphosphinate as Versatile Building Blocks To Design all Inorganic Coordination Polymers. Inorganic Chemistry, 2017, 56, 5502-5505.	4.0	22
60	Structural Relationships obtained from the Coordination of α-Picolinamide to the (Iminodiacetato)copper(II) Chelate: Synthesis, Crystal Structure, and Properties of (α-Picolinamide)(iminodiacetato)copper(II) Dihydrate. Zeitschrift Fur Anorganische Und Allgemeine Chemie, 2000, 626, 930-936.	1.2	21
61	Two intra-molecular inter-ligand C(aromatic)–Hâ⊂O(carboxyl) interactions reinforce the formation of a single Cu(II)–N4(nza) bond in the molecular recognition between pyrazine-2-carboxamide (nza) and	3.9	21
62	Amide-tethered organosilatranes: Syntheses, structural characterization and photophysical properties. Inorganica Chimica Acta, 2015, 433, 78-91.	2.4	20
63	Photoluminescence in <i>m</i> -carborane–anthracene triads: a combined experimental and computational study. Journal of Materials Chemistry C, 2018, 6, 11336-11347.	5.5	20
64	Efficient blue light emitting materials based on <i>m</i> -carborane–anthracene dyads. Structure, photophysics and bioimaging studies. Biomaterials Science, 2019, 7, 5324-5337.	5.4	20
65	Interligand ï€,ï€-stacking interactions giving a bi-layered 2D framework in the crystal of poly-{(N4′-2,4′-bipyridine)-μ-(N,O,O′,O″-iminodiacetato)copper(II) hydrate}, {[Cu(IDA)(2,4′-bipy)]Â Inorganic Chemistry Communication, 2003, 6, 343-345.	\• ม 2O}n.	19
66	3dâ^'3dâ^'4f Chain Complexes Constructed Using the Dinuclear Metallacyclic Complex [Ni ₂ (mbpb) ₃] ^{2â^'} [H ₂ mbpb = 1,3-Bis(pyridine-2-carboxamide)benzene] as a Ligand: Synthesis, Structures, and Magnetic Properties. Inorganic Chemistry, 2010, 49, 1826-1833.	4.0	19
67	Chelating Ligand Conformation Driving the Hypoxanthine Metal Binding Patterns, Inorganic	4.0	19
68	From 7-azaindole to adenine: molecular recognition aspects on mixed-ligand Cu(ii) complexes with deaza-adenine ligands. Dalton Transactions, 2013, 42, 6119.	3.3	19
69	Synthesis and structural characterization of 2-D layered copper(II) styrylphosphonate coordination polymers. Journal of Coordination Chemistry, 2014, 67, 1562-1572.	2.2	19
70	Lights and shadows in the challenge of binding acyclovir, a synthetic purine-like nucleoside with antiviral activity, at an apical–distal coordination site in copper(II)-polyamine chelates. Journal of Inorganic Biochemistry, 2015, 148, 84-92.	3.5	19
71	Three-Component Copper-Phosphonate-Auxiliary Ligand Systems: Proton Conductors and Efficient Catalysts in Mild Oxidative Functionalization of Cycloalkanes. Inorganic Chemistry, 2018, 57, 10656-10666.	4.0	19
72	On/off electrochemical switches based on quinone-bisketals. Chemical Communications, 2011, 47, 1586-1588.	4.1	18

#	ARTICLE	IF	CITATIONS
73	Heterometallic Oximatoa€Bridged Linear Trinuclear Ni ^{li} a Mi ^{lii} a Ni ^{lii}	e): A 2.0	18
74	Molecular recognition patterns of 2-aminopurine versus adenine: A view through ternary copper(II) complexes. Journal of Inorganic Biochemistry, 2011, 105, 1073-1080.	3.5	18
75	Is Molecular Chirality Connected to Supramolecular Chirality? The Particular Case of Chiral 2-Pyridyl Alcohols. Crystal Growth and Design, 2015, 15, 935-945.	3.0	17
76	Growth Behavior of Monohydrocalcite (CaCO3·H2O) in Silica-Rich Alkaline Solution. Crystal Growth and Design, 2015, 15, 564-572.	3.0	17
77	Luminescence properties of carborane-containing distyrylaromatic systems. Journal of Organometallic Chemistry, 2018, 865, 206-213.	1.8	17
78	Slow-spin relaxation of a low-spin S = 1/2 FeIII carborane complex. Chemical Communications, 2019, 55, 3825-3828.	4.1	17
79	The unexpected tridentate role of the tripodal ligand N-(carbamoylmethyl)iminodiacetato(2â^') (ADA) in a new mixed-ligand nickel(II) complex with 2,2′-bipyridine (bipy) as secondary ligand: structure of [Ni(ADA)(bipy)(H2O)]·4H2O. Inorganic Chemistry Communication, 2002, 5, 727-729.	3.9	16
80	Synthesis and Crystallographic Studies of Disubstituted Carboranyl Alcohol Derivatives: Prevailing Chiral Recognition?. Crystal Growth and Design, 2013, 13, 1473-1484.	3.0	16
81	Stereospecific alkylation of substituted adenines by the Mitsunobu coupling reaction under microwave-assisted conditions. RSC Advances, 2014, 4, 22425-22433.	3.6	16
82	Incorporation of azo group at axial position of silatranes: synthesis, characterization and antimicrobial activity. Applied Organometallic Chemistry, 2015, 29, 549-555.	3.5	16
83	A double basic Sr-amino containing MOF as a highly stable heterogeneous catalyst. Dalton Transactions, 2019, 48, 11556-11564.	3.3	16
84	MOF transmetalation beyond cation substitution: defective distortion of IRMOF-9 in the spotlight. CrystEngComm, 2019, 21, 827-834.	2.6	16
85	Tuning the architectures and luminescence properties of Cu(<scp>i</scp>) compounds of phenyl and carboranyl pyrazoles: the impact of 2D <i>versus</i> 3D aromatic moieties in the ligand backbone. Journal of Materials Chemistry C, 2021, 9, 7643-7657.	5.5	16
86	A structural evidence for the preferential coordination of the primary amide group versus the unionised carboxyl group: synthesis, molecular and crystal structure, and properties of [Cu(HADA)2], a new copper(II) bis-chelate (H2ADA=N-(2-carbamoyImethyl)iminodiacetic acid). Inorganic Chemistry Communication, 2003, 6, 71-73.	3.9	15
87	Zinc(II) and copper(II) complexes with hydroxypyrone iron chelators. Journal of Inorganic Biochemistry, 2015, 151, 94-106.	3.5	15
88	Precipitation and Crystallization Kinetics in Silica Gardens. ChemPhysChem, 2017, 18, 338-345.	2.1	15
89	Restricting the versatile metal-binding behaviour of adenine by using deaza-purine ligands in mixed-ligand copper(II) complexes. Polyhedron, 2010, 29, 170-177.	2.2	14
90	Strasseriolides A–D, A Family of Antiplasmodial Macrolides Isolated from the Fungus Strasseria geniculata CF-247251. Organic Letters, 2020, 22, 6709-6713.	4.6	14

#	Article	IF	CITATIONS
91	The first metal chelate of un-substituted 2,6-pyridine-dicarboxamide (pdcam): synthesis, molecular and crystal structure, and properties of [Cull(pdc)(pdcam)]·2H2O (pdc=2,6-pyridine-dicarboxylato(2â^')) Tj ETQq1	1 0 <i>3</i> . 9 4314	⊦rgƁT /Overle
92	Interconvertible Hydrochlorothiazide–Caffeine Multicomponent Pharmaceutical Materials: A Solvent Issue. Crystals, 2020, 10, 1088.	2.2	13
93	Water soluble organometallic small molecules as promising antibacterial agents: synthesis, physical–chemical properties and biological evaluation to tackle bacterial infections. Dalton Transactions, 2022, 51, 7188-7209.	3.3	13
94	Crystallization of monohydrocalcite in a silica-rich alkaline solution. CrystEngComm, 2013, 15, 6526.	2.6	12
95	Cyanide-bridged tetradecanuclear Rull3Mll11 clusters (Mll = Znll and Cull) based on the high connectivity building block [Ru3(HAT)(CN)12]6â^': structural and photophysical properties. Chemical Communications, 2008, , 4460.	4.1	11
96	Molecular recognition modes between adenine or adeniniun(1+) ion and binary MII(pdc) chelates (MCoZn; pdc=pyridine-2,6-dicarboxylate(2-) ion). Journal of Inorganic Biochemistry, 2013, 127, 211-219.	3.5	11
97	A New Kind of Quinonic-Antibiotic Useful Against Multidrug-Resistant S. aureus and E. faecium Infections. Molecules, 2018, 23, 1776.	3.8	11
98	2-Aminopyrimidinium Decavanadate: Experimental and Theoretical Characterization, Molecular Docking, and Potential Antineoplastic Activity. Inorganics, 2021, 9, 67.	2.7	11
99	Enantiospecific Synthesis of Heterocycles Linked to Purines: Different Apoptosis Modulation of Enantiomers in Breast Cancer Cells. Current Medicinal Chemistry, 2013, 20, 4924-4934.	2.4	11
100	Rational design of carborane-based Cu ₂ -paddle wheel coordination polymers for increased hydrolytic stability. Dalton Transactions, 2022, 51, 1137-1143.	3.3	11
101	Metal binding pattern of acyclovir in ternary copper(II) complexes having an S-thioether or S-disulfide NO2S-tripodal tetradentate chelator. Inorganica Chimica Acta, 2016, 452, 258-267.	2.4	10
102	Extensive analysis of N—HO hydrogen bonding in four classes of phosphorus compounds: a combined experimental and database study. Acta Crystallographica Section C, Structural Chemistry, 2017, 73, 287-297.	0.5	10
103	O–H and (CO)N–H bond weakening by coordination to Fe(<scp>ii</scp>). Dalton Transactions, 2019, 48, 2179-2189.	3.3	10
104	Platonic Relationships in Metal Phosphonate Chemistry: Ionic Metal Phosphonates. Crystals, 2019, 9, 301.	2.2	10
105	Optimization and comparison of statistical tools for the prediction of multicomponent forms of a molecule: the antiretroviral nevirapine as a case study. CrystEngComm, 2020, 22, 7460-7474.	2.6	10
106	Anti-cancer and anti-inflammatory activities of a new family of coordination compounds based on divalent transition metal ions and indazole-3-carboxylic acid. Journal of Inorganic Biochemistry, 2021, 215, 111308.	3.5	10
107	Furosemide/Non-Steroidal Anti-Inflammatory Drug–Drug Pharmaceutical Solids: Novel Opportunities in Drug Formulation. Crystals, 2021, 11, 1339.	2.2	10
108	A novel Zn-based-MOF for efficient CO2 adsorption and conversion under mild conditions. Catalysis Today, 2022, 390-391, 230-236.	4.4	10

#	Article	IF	CITATIONS
109	Calcium and Strontium Coordination Polymers as Controlled Delivery Systems of the Anti-Osteoporosis Drug Risedronate and the Augmenting Effect of Solubilizers. Applied Sciences (Switzerland), 2021, 11, 11383.	2.5	10
110	Synthesis and reactivity of (RS)-6-chloro-7- or 9-(1,2,3,5-tetrahydro-4,1-benzoxazepin-3-yl)-7H- or 9H-purines bearing a nitrobenzenesulfonyl group on the nitrogen atom. Tetrahedron, 2007, 63, 5274-5286.	1.9	9
111	A redetermination of (N9-adenine-κN)aqua[glycylglycinato(2â^')-κ3N,N′,O]copper(II). Acta Crystallographica Section E: Structure Reports Online, 2007, 63, m1598-m1598.	0.2	9
112	Cocrystallization of Mononuclear and Trinuclear Metallacycle Molecules from an Aqueous Mixed-Ligand Copper(II) Solution. Crystal Growth and Design, 2014, 14, 889-892.	3.0	9
113	Carboranylphosphinic Acids: A New Class of Purely Inorganic Ligands. Chemistry - A European Journal, 2016, 22, 3665-3670.	3.3	9
114	Two new phosphinic amides: Synthesis, crystal structure, and theoretical study of hydrogen bonding. Phosphorus, Sulfur and Silicon and the Related Elements, 2017, 192, 359-367.	1.6	9
115	New Multicomponent Forms of the Antiretroviral Nevirapine with Improved Dissolution Performance. Crystal Growth and Design, 2020, 20, 688-698.	3.0	9
116	Supramolecular architectures of Mn(NCS)2 complexes with N'-(1-(pyridin-4-yl)ethylidene)picolinohydrazide and N'-(phenyl(pyridin-4-yl)methylene)isonicotinohydrazide. Polyhedron, 2020, 190, 114776.	2.2	9
117	Interpenetrated Luminescent Metal–Organic Frameworks based on 1 <i>H</i> -Indazole-5-carboxylic Acid. Crystal Growth and Design, 2020, 20, 4550-4560.	3.0	9
118	Novel Polymorphic Cocrystals of the Non-Steroidal Anti-Inflammatory Drug Niflumic Acid: Expanding the Pharmaceutical Landscape. Pharmaceutics, 2021, 13, 2140.	4.5	9
119	Mixed-ligand Complexes with 2,6-Pyridinedicarboxylato(2-) and 4,7-Diphenyl-1,10-Phenanthroline Ligands, [MII(pdc)(DPphen)(H2O)]·H2O (M = Co or Cu). Synthesis, Crystal Structures and Properties. Zeitschrift Fur Anorganische Und Allgemeine Chemie, 2005, 631, 2081-2085.	1.2	8
120	Ternary copper(II) complexes with N-carboxymethyl-l-prolinato(2â^') ion and imidazole or creatinine: A comparative study of the interligand interactions influencing the molecular recognition and stability. Journal of Inorganic Biochemistry, 2005, 99, 1424-1432.	3.5	8
121	Nickel(II) derivatives of N-benzyliminodiacetate(2â^') ligands, with and without imidazole: Synthesis, crystal structure and properties. Polyhedron, 2010, 29, 683-690.	2.2	8
122	Synthesis, spectroscopic, and thermal analyses of binuclear mixed ligand Co(II) and Ni(II) complexes. Journal of Coordination Chemistry, 2011, 64, 1544-1553.	2.2	8
123	A new 2D cadmium chloride network with 2-aminopyrimidine displaying long lifetime photoluminescence emission. Polyhedron, 2011, 30, 1295-1298.	2.2	8
124	Substituted phenyl urea and thiourea silatranes: Synthesis, characterization and anion recognition properties by photophysical and theoretical studies. Polyhedron, 2016, 112, 51-60.	2.2	8
125	Novel and Versatile Cobalt Azobenzeneâ€Based Metalâ€Organic Framework as Hydrogen Adsorbent. ChemPhysChem, 2019, 20, 1334-1339.	2.1	8
126	Designing Single-Molecule Magnets as Drugs with Dual Anti-Inflammatory and Anti-Diabetic Effects. International Journal of Molecular Sciences, 2020, 21, 3146.	4.1	8

#	Article	IF	CITATIONS
127	Eu-Doped Citrate-Coated Carbonated Apatite Luminescent Nanoprobes for Drug Delivery. Nanomaterials, 2020, 10, 199.	4.1	8
128	Crystallization, Luminescence and Cytocompatibility of Hexagonal Calcium Doped Terbium Phosphate Hydrate Nanoparticles. Nanomaterials, 2021, 11, 322.	4.1	8
129	Exploiting the Multifunctionality of M ²⁺ /Imidazole–Etidronates for Proton Conductivity (Zn ²⁺) and Electrocatalysis (Co ²⁺ , Ni ²⁺) toward the HER, OER, and ORR. ACS Applied Materials & Interfaces, 2022, 14, 11273-11287.	8.0	8
130	Substituent effects on the reaction mode between 2-hydroxybenzyl alcohol derivatives and MEM chloride: synthesis and mechanistic aspects of seven- and ten-membered benzo-fused O,O-acetals. Tetrahedron, 2004, 60, 11453-11464.	1.9	7
131	A Structural Study of the Iminodiacetate Moiety Conformation in N-(1-adamantyl)-iminodiacetate(2-) Copper(II) Complexes. Zeitschrift Fur Anorganische Und Allgemeine Chemie, 2007, 633, 2658-2666.	1.2	7
132	Spectroscopic, structural and magnetic studies of nickel(II) complexes with tetra- and pentadentate ligands. Transition Metal Chemistry, 2009, 34, 239-245.	1.4	7
133	Structural Consequences of the N7 and C8 Translocation on the Metal Binding Behavior of Adenine. Inorganic Chemistry, 2013, 52, 1916-1925.	4.0	7
134	Synthesis, structures and properties of ironIII complexes with (o-carboranyl)bis-(2-hydroxymethyl)pyridine: Racemic versus meso. Inorganica Chimica Acta, 2016, 448, 97-103.	2.4	7
135	Switchable Surface Hydrophobicity–Hydrophilicity of a Metal–Organic Framework. Angewandte Chemie, 2016, 128, 16283-16287.	2.0	7
136	Copper(II) polyamine chelates as efficient receptors for acyclovir: syntheses, crystal structures and dft study. Polyhedron, 2018, 145, 218-226.	2.2	7
137	Cysteine-based 3-substituted 1,5-benzoxathiepin derivatives: Two new classes of anti-proliferative agents. Arabian Journal of Chemistry, 2018, 11, 426-441.	4.9	7
138	Slow relaxation of magnetization and luminescence properties of a novel dysprosium and pyrene-1,3,6,8-tetrasulfonate based MOF. New Journal of Chemistry, 2018, 42, 832-837.	2.8	7
139	A Reversible Phase Transition of 2D Coordination Layers by B–Hâ^™â^™â^™Cu(II) Interactions in a Coordination Polymer. Molecules, 2019, 24, 3204.	3.8	7
140	In vitro evaluation of leishmanicidal properties of a new family of monodimensional coordination polymers based on diclofenac ligand. Polyhedron, 2020, 184, 114570.	2.2	7
141	Phase Transformation Dynamics in Sulfate-Loaded Lanthanide Triphosphonates. Proton Conductivity and Application as Fillers in PEMFCs. ACS Applied Materials & amp; Interfaces, 2021, 13, 15279-15291.	8.0	7
142	Luminescent Citrate-Functionalized Terbium-Substituted Carbonated Apatite Nanomaterials: Structural Aspects, Sensitized Luminescence, Cytocompatibility, and Cell Uptake Imaging. Nanomaterials, 2022, 12, 1257.	4.1	7
143	Metal Chelates of N-(2-pyridylmethyl)iminodiacetate(2-) Ion (pmda). Part II. Ternary pmda Chelates with M = Co, Cu or Zn and Creatinine as Auxiliary Ligand. Zeitschrift Fur Anorganische Und Allgemeine Chemie, 2006, 632, 845-850.	1.2	6
144	Structural insights on the molecular recognition patterns between N6-substituted adenines and N-(aryl-methyl)iminodiacetate copper(II) chelates. Journal of Inorganic Biochemistry, 2013, 127, 141-149.	3.5	6

#	Article	IF	CITATIONS
145	Synthesis, thermogravimetric study and crystal structure of an N-rich copper(II) compound with tren ligands and nitrate counter-anions. Thermochimica Acta, 2014, 593, 7-11.	2.7	6
146	Highest Reported Denticity of a Synthetic Nucleoside in the Unprecedented Tetradentate Mode of Acyclovir. Crystal Growth and Design, 2018, 18, 4282-4286.	3.0	6
147	Rational design of an unusual 2D-MOF based on Cu(<scp>i</scp>) and 4-hydroxypyrimidine-5-carbonitrile as linker with conductive capabilities: a theoretical approach based on high-pressure XRD. Chemical Communications, 2020, 56, 9473-9476.	4.1	6
148	Synthesis, Structural Features, and Hydrogen Adsorption Properties of Three New Flexible Sulfur-Containing Metal–Organic Frameworks. Crystal Growth and Design, 2020, 20, 6707-6714.	3.0	6
149	Anthracene–styrene-substituted <i>m</i> -carborane derivatives: insights into the electronic and structural effects of substituents on photoluminescence. Inorganic Chemistry Frontiers, 2020, 7, 2370-2380.	6.0	6
150	A gliclazide complex based on palladium towards Alzheimer's disease: promising protective activity against Aβ-induced toxicity in <i>C. elegans</i> . Chemical Communications, 2022, 58, 1514-1517.	4.1	6
151	Catalytic Performance and Electrophoretic Behavior of an Yttrium–Organic Framework Based on a Tricarboxylic Asymmetric Alkyne. Inorganic Chemistry, 2022, 61, 1377-1384.	4.0	6
152	Mixed-ligand Copper(II) Complexes with N-isopropyl-iminodiacetato(2-) and C-phenyl-imidazole Ligands. Crystal Structures of H2iPIDA, [Cu(iPIDA)(H2݆im)(H2O)]·3H2O and [Cu(iPIDA)(H5݆im)]n. Zeitschrift Fur Anorganische Und Allgemeine Chemie, 2005, 631, 2156-2160.	1.2	5
153	Dinuclear EGTA-copper(II) chelates with imidazole as auxiliary ligand. Inorganic Chemistry Communication, 2006, 9, 903-906.	3.9	5
154	cis-[N-(4-Chlorobenzyl)iminodiacetato-κ3N,O,Oâ€2]bis(1H-imidazole-κN3)copper(II). Acta Crystallographica Section E: Structure Reports Online, 2007, 63, m1678-m1679.	0.2	5
155	Molecular recognition between adenine or 2,6-diaminopurine and copper(II) chelates with N,O2,S-tripodal tetradentate chelators having thioether or disulfide donor groups. Journal of Inorganic Biochemistry, 2015, 151, 75-86.	3.5	5
156	Molecular and supramolecular recognition patterns in ternary copper(II) or zinc(II) complexes with selected rigid-planar chelators and a synthetic adenine-nucleoside. Journal of Inorganic Biochemistry, 2020, 203, 110920.	3.5	5
157	Magnetic and Luminescent Properties of Isostructural 2D Coordination Polymers Based on 2-Pyrimidinecarboxylate and Lanthanide Ions. Crystals, 2020, 10, 571.	2.2	5
158	Combined experimental and theoretical investigation on the magnetic properties derived from the coordination of 6-methyl-2-oxonicotinate to 3d-metal ions. Dalton Transactions, 2022, 51, 9780-9792.	3.3	5
159	Unsymmetrically urea silatranes: Synthesis, characterization and a selective on–off fluorescence response to acetate anion. Arabian Journal of Chemistry, 2017, 10, 523-531.	4.9	4
160	Crystalline Inclusion Compounds of a Palladacyclic Tetraol Host Featuring <i>o</i> arborane Units. European Journal of Inorganic Chemistry, 2017, 2017, 4589-4598.	2.0	4
161	5-Aminopyridine-2-carboxylic acid as appropriate ligand for constructing coordination polymers with luminescence, slow magnetic relaxation and anti-cancer properties. Journal of Inorganic Biochemistry, 2020, 207, 111051.	3.5	4
162	Lidocaine Pharmaceutical Multicomponent Forms: A Story about the Role of Chloride Ions on Their Stability. Crystals, 2022, 12, 798.	2.2	4

#	Article	IF	CITATIONS
163	¹ H, ¹³ C NMR, Xâ€ray and conformational studies of new 1â€alkylâ€3â€benzoylâ€pyra and 1â€alkylâ€3â€benzoylâ€pyrazoline derivatives. Magnetic Resonance in Chemistry, 2008, 46, 878-885.	azolg 1.9	3
164	Two tautomeric polymorphs of 2,6-dichloropurine. Acta Crystallographica Section C: Crystal Structure Communications, 2011, 67, o484-o486.	0.4	3
165	Characterization of 4,5-Dihydro-1H -Pyrazole Derivatives by 13 C NMR Spectroscopy. Magnetic Resonance in Chemistry, 2012, 50, 58-61.	1.9	3
166	Looking at new ligands for chelation therapy. New Journal of Chemistry, 2018, 42, 8021-8034.	2.8	3
167	Dicopper(II)-EDTA Chelate as a Bicephalic Receptor Model for a Synthetic Adenine Nucleoside. Pharmaceuticals, 2021, 14, 426.	3.8	3
168	A Mixed Heterobimetallic Y/Eu-MOF for the Cyanosilylation and Hydroboration of Carbonyls. Catalysts, 2022, 12, 299.	3.5	3
169	(2,3-Dihydro-1,4-benzodioxin-2-yl)methanol. Acta Crystallographica Section E: Structure Reports Online, 2007, 63, o2940-o2940.	0.2	2
170	Synthesis, crystal structure and properties of three different derivatives of bis[di(2-pyridyl)methanediol]copper(II), [Cu(bpmd) ₂] ²⁺ . Journal of Coordination Chemistry, 2009, 62, 120-129.	2.2	2
171	<i>trans</i> -Diaquabis(<scp>L</scp> -phenylalaninato-κ ² <i>N</i> , <i>O</i>)nickel(II). Acta Crystallographica Section E: Structure Reports Online, 2012, 68, m446-m446.	0.2	2
172	Isotype 1D polymers of cobalt(II) or zinc(II) constructed with square-planar tetraaqua-metal(2+) units and the bis-zwitterionic form of the μ2-O,O′-trans-1,4-dihydrogen-cyclohexanediaminotetraacetate(2â^') ligand. Polyhedron, 2012, 31, 463-471.	2.2	2
173	Synthesis and Characterization of Zinc(II) and Cadmium(II) Mixed Ligand Trichloroacetate Complexes. Synthesis and Reactivity in Inorganic, Metal Organic, and Nano Metal Chemistry, 2013, 43, 283-288.	0.6	2
174	NMR assignments and structural characterization of new thiourea and urea kynurenamine derivatives nitric oxide synthase inhibitors. Magnetic Resonance in Chemistry, 2015, 53, 1071-1079.	1.9	2
175	Two Isostructural URJC-4 Materials: From Hydrogen Physisorption to Heterogeneous Reductive Amination through Hydrogen Molecule Activation at Low Pressure. Inorganic Chemistry, 2020, 59, 15733-15740.	4.0	2
176	Dimeric metallacycles and coordination polymers: Zn(II), Cd(II) and Hg(II) complexes of two positional isomers of a flexible N,O-hybrid bispyrazole derived ligand. Inorganica Chimica Acta, 2020, 506, 119549.	2.4	2
177	Broadening the scope of high structural dimensionality nanomaterials using pyridine-based curcuminoids. Dalton Transactions, 2021, 50, 7056-7064.	3.3	2
178	Biomimetic Citrate-Coated Luminescent Apatite Nanoplatforms for Diclofenac Delivery in Inflammatory Environments. Nanomaterials, 2022, 12, 562.	4.1	2
179	Tris(2-Pyridylmethylamine)V(O)2 Complexes as Counter Ions of Diprotonated Decavanadate Anion: Potential Antineoplastic Activity. Frontiers in Chemistry, 2022, 10, 830511.	3.6	2
180	Through-space hopping transport in an iodine-doped perylene-based metal–organic framework. Molecular Systems Design and Engineering, 2022, 7, 1065-1072.	3.4	2

#	Article	IF	CITATIONS
181	NMR spectroscopic characterization of new 2,3â€dihydroâ€1,3,4â€thiadiazole derivatives. Magnetic Resonance in Chemistry, 2012, 50, 515-522.	1.9	1
182	Unprecedented 4/5-methylimidazole linkage isomerism within a binuclear copper(II) complex molecule. Inorganic Chemistry Communication, 2014, 42, 20-22.	3.9	1
183	Synthesis, X-Ray Structure and Anti-Bacterial Studies of 1,3-Thiazolylpropylsilatranes. Phosphorus, Sulfur and Silicon and the Related Elements, 2015, 190, 1971-1979.	1.6	1
184	Monoclinic and orthorhombic forms of (<i>RS</i>)-(<i>E</i>)-4-[2-(4-chlorobenzylidene)hydrazinyl]-6,11-dimethyl-6,11-dihydro-5 <i>H</i> -benzo[<i>b</i> synthesis, concomitant polymorphism and supramolecular assembly mediated by Câ€"HN, Câ€"HI€(arene) and Câ€"ClI€(arene) interactions. Acta Crystallographica Section C, Structural]pyrimido 0.5	[5,4- <i>f1</i>
185	Chemistry, 2019, 75, 686-693. Vapour Diffusion Sitting Drop Method to Induce Nucleation of Calcium Phosphate on Exfoliated Graphene and Graphene Oxide Flakes. Crystals, 2021, 11, 767.	2.2	1
186	Structure of the first dinuclear Ni(II) complex with an azapurine derivative (the anionic form of) Tj ETQq0 0 0 rgBT 1081-1084.	/Overlock 3.9	10 Tf 50 54 0
187	Metal complexes with N-(trifluoromethylbenzyl)iminodiacetate chelators (x-3F ligands). Part I. Copper(II) chelates of p-3F, m-3F, and o-3F with or without imidazole-like ligands. Journal of Coordination Chemistry, 2015, 68, 2739-2759.	2.2	0
188	Photoluminescence and in vitro cytotoxicity analysis in a novel mononuclear Zn(II) coordination compound based on bumetanide. Inorganica Chimica Acta, 2020, 509, 119708.	2.4	0
189	Crystal structure and Hirshfeld surface analysis of diiodido{ <i>N</i> ′-[(<i>E</i>)-(phenyl)(pyridin-2-yl-l° <i>N</i>)methylidene]pyridine-2-carbohydrazide-l° ^{2- <i>N</i>′,<i>O</i>}cadmium(II). Acta Crystallographica Section E: Crystallographic Communications, 2019. 75. 1061-1064.}	(sup>	0
190	Selectivity of Relative Humidity Using a CP Based on S-Block Metal Ions. Sensors, 2022, 22, 1664.	3.8	0
191	INTERLABORATORY VIRTUAL COLLABORATIVE EXPERIENCES IN CHEMISTRY LABS. INTED Proceedings, 2022, , .	0.0	0
192	Sensing Capacity in Dysprosium Metal–Organic Frameworks Based on 5-Aminoisophthalic Acid Ligand. Sensors, 2022, 22, 3392.	3.8	0